IEEJ Journal of Industry Applications
Vol.4 No.2 pp.91–97 DOI: 10.1541/ieejjia.4.91

Paper

A Feasibility Study on Multiple Frequency CW for Landing Radar

Manabu Akita[*a)] Member, Daisuke Nakashima[*] Non-member
Masato Watanabe[*] Non-member, Takayuki Inaba[*] Non-member

(Manuscript received March 12, 2014, revised Sep. 14, 2014)

Landing radar that measures the velocity and the altitude of the airframe has been developed for the sensor, which helps safe landing. In applications where the observation range is limited to a very short range such as the final stage of landing, we can expect to obtain a high signal-to-noise (S/N) ratio. In these situations, the multiple frequency continuous wave (CW) with MUSIC (MUltiple SIgnal Classification) algorithm is considered to be useful for achieving a high resolution with a low sampling rate of several tens of kilohertz and relatively low-speed signal processing. In this paper, the multiple frequency CW with 1D and 2D MUSIC algorithm to measure the altitude is described. The simulation shows that the bias errors in both methods are less than 1% of the altitudes. The random errors of 1D MUSIC and 2D MUSIC are 1.3%–1.7% and 0.8%–1.0%, respectively. The random errors of 2D MUSIC are smaller than those of 1D MUSIC. We also show the fundamental experimental results obtained in an athletic field using the radar fitted on a cage lifted by a crane. We could obtain stable estimation results on altitudes between 1.0 m and 7.0 m. These results indicate that the multiple frequency CW radar is one of the effective tools for landing radar in the final phase of landing.

Keywords: radar, remote sensing, altimeter, multiple frequency CW

1. Introduction

Radar is applied to various usages such as meteorological measurements and air traffic controls, since it is able to measure the relative velocity of the targets directly. Radar is also applied to the altimeter for airframes [(1)]. The landing radar measuring the velocity and the distance between airframe and the ground surface has been developing for the sensor which helps safe landing. The advantages of use of radar for this purpose are as follows. Radar is robust to dust and has good weather resistance comparing to laser and other optical measurements. Landing radar has been developed for helicopters and exploration spacecrafts. Such airframes generate dense dust on the unprepared terrain. Radar can also work even if the attitude of airframe changes, since radar has wide view of angle. The landing radar is required to be able to measure the velocity and altitude from the altitude of several thousand meters to a few meters. Pulse compression and short pulse radars are used in high and low altitude in the descent stage of landing, respectively [(2)]. However, short pulse radar faces the transmitter-to-receiver isolation problem in the final phase of landing at altitude of about 10 m or less [(3)]. Furthermore, a high range resolution is also required especially at the low altitude in the final phase of landing.

In this paper, we apply multiple frequency continuous wave (CW), which can mitigate the transmitter-to-receiver isolation problem and has a high range resolution, as a radar modulation for the final phase of landing. The multiple frequency CW employs CW for transmission signal instead of pulsed signal in multiple frequency ICW [(4)]. The multiple frequency CW is based on ranging technique which uses phase differences of detected Doppler frequency at carrier frequencies and the accuracy depends on the signal-to-noise (S/N) ratio. In applications where the observation range is limited to very short range such as the final stage of landing, we can expect to obtain high S/N ratio. Multiple frequency CW with a super-resolution algorithm such as MUSIC (MUltiple SIgnal Classification) also improves the isolation between the targets having the same Doppler frequency, which is one of the advantages in the situations where the observation targets are composed of many reflection points. The improvement of target isolation that distinguishes the signal component associated with the ground right below the airframe from the signal components associated with the surrounding area is also important for measuring the shortest distance to the ground (altitude). Thus the method is suitable for radar modulation for short range and enables us to obtain a high range resolution with a low sampling rate of several tens of kilohertz and relatively low-speed signal processing. The modification does not require a high peak power owing to adopting CW. Therefore the modification can be achieved at low cost and save power. Our research group has conducted a feasibility study on the method for middle-range automotive radar [(5)].

In this paper, we conduct feasibility study on multiple frequency CW for landing radar of the airframes that descends right down to the ground such as exploration spacecrafts. In this process, we adopt 2D MUSIC algorism [(6)] on the multiple frequency CW to obtain not only a high range resolution but also a high velocity resolution. At first, we describe the

a) Correspondence to: Manabu Akita. E-mail: akita.manabu@uec.ac.jp
* Graduate School of Informatics and Engineering, The University of Electro-Communications
1-5-1, Choufugaoka, Choufu-shi, Tokyo 182-8585, Japan

multiple frequency CW with 1D and 2D MUSIC. Then we show the simulation results for the situation where the radar is equipped on an airframe. We also show the experimental results obtained in an athletic field using the radar equipped on a cage lifted by a crane.

2. Methods

2.1 Observed Signal of Multiple Frequency CW

Figure 1 shows the transmission frequency sequence of multiple frequency CW. In this method, the same sequence where the carrier frequency $f_n (n = 0, 1, \cdots N-1)$ is switched N times every T_{pri} is repeated M times in 1 CPI ($T_c = MNT_{pri}$). Here the transmission signal is described as

$$T_n(t) = \exp\left[j\left(2\pi\left(f_n t\right) + \phi_n\right)\right], \cdots\cdots\cdots\cdots\cdots (1)$$

where ϕ_n are given as initial phases. The received signal from a single target is described as

$$R_n(t) = a_0 \exp\left[j\left(2\pi\left(f_n + f_{d,n}\right)t - \frac{4\pi f_n}{c}R + \phi_n\right)\right], \cdots\cdots\cdots\cdots\cdots (2)$$

where the wave lengths of nth carrier frequencies (f_n) correspond to $\frac{c}{f_n}$, and $f_{d,n}$ are Doppler frequencies at nth carrier frequencies. c is speed of light. R is the range of the target. a_0 represents the amplitude that depends on the backward scattering coefficient and range of the target, which is explained in Sect. 3.1. The received signal is mixed with transmission signal and then the observation signal is obtained. The observation signal is described by

$$X_n(t) = a_0 \exp\left[j\left(2\pi f_{d,n}t - \frac{4\pi f_n}{c}R\right)\right] \cong a_0 \exp\left[j\left(2\pi f_d t - \frac{4\pi f_n}{c}R\right)\right] \cdots\cdots\cdots\cdots\cdots (3)$$

where we can assume that $f_{d,n}$ take almost same values, since the differences of carrier frequencies $n\cdot\Delta f\,(n = 0, 1, \cdots N-1)$ are negligible small compared to the carrier frequency (f_0).

$$f_{d,n}(n = 0, 1, \cdots N-1) \cong f_d \cdots\cdots\cdots\cdots\cdots (4)$$

The received signal is sampled at the middle time of each frequency. The sampling time $t_{n,m}$ is also described by

$$t_{n,m} = T_{PRI}n + T_{PRI}N\cdot m + \frac{1}{2}T_{PRI}, \cdots\cdots\cdots\cdots (5)$$

where $m(m = 0, 1, \cdots M-1)$ is repetitive number of transmission sequence. The observed signal is also expressed by

$$X(n,m) = a_0 \exp\left[j\left(2\pi f_d T_{PRI}(n + N\cdot m) - \frac{4\pi f_n}{c}R + \pi f_d T_{PRI}\right)\right]$$
$$= a_0 \exp\left[j\left(2\pi f_d T_{PRI}N\cdot m + (2\pi f_d T_{PRI} - \frac{4\pi\Delta f}{c}R)\cdot n - \frac{4\pi f_0}{c}R + \pi f_d T_{PRI}\right)\right]. \cdots\cdots\cdots\cdots\cdots (6)$$

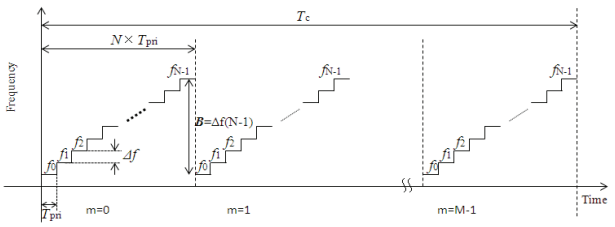

Fig. 1. Transmit and receive timing of multiple frequency CW

In multiple target situations, the observation signal is expressed by the linear summations of the Eq. (6).

2.2 Multiple Frequency CW with 1D MUSIC

In this section, the signal processing of multiple frequency CW with 1D MUSIC for the target detection, calculating velocity and altitude is described.

2.2.1 Signal Processing for the Target Velocity

The target velocity is calculated by executing FFT on the observation signal (M length) at nth carrier frequency,

$$E(n,k) = \sum_{m=0}^{M-1} X(n,m)\exp\left[-2\pi j\left(\frac{m}{M}k\right)\right], \cdots\cdots\cdots (7)$$

where $k\,(= 0, 1, \cdots M-1)$ corresponds to the number proportional to the Doppler frequency. $|E(n,k)|$ take local maximum values at k_{peak}, which is expressed by

$$k_{peak} = f_d T_{PRI} MN. \cdots\cdots\cdots\cdots\cdots (8)$$

The Doppler frequencies of targets are obtained by detecting k_{peak} where $|E(n,k)|$ take local maximum values. The target velocity is also calculated by

$$\hat{V} = f_d\frac{\lambda}{2} = \frac{k_{peak}}{T_{PRI}MN}\frac{\lambda}{2}. \cdots\cdots\cdots\cdots (9)$$

$E(n, k_{peak})$ is expressed by

$$E(n,k_{peak}) \cong A_{peak}\exp\left[j\left(\left(2\pi\frac{k_{peak}}{MN} - \frac{4\pi\Delta f}{c}R\right)\cdot n - \frac{4\pi f_0}{c}R + \pi f_d T_{PRI}\right)\right]. \cdots\cdots\cdots (10)$$

A_{peak} represents the amplitude associated with a target. In the situation where the airframe equipped with the radar descends to the ground, $|E(n,k)|$ is possible to have multiple peaks, since the ground is composed of multiple reflection points. The received signal from the ground just below the airframe is considered to have the maximum Doppler frequency. Thus the maximum frequency where the amplitude exceeds a given threshold level and takes the local maximum value is assumed to be associated with the relative velocity between the airframe and the ground. In this method, the threshold is set to 3 dB lower than the maximum value.

2.2.2 Signal Processing for the Altitude Measurement

The range of target can be calculated by using the slope of phase difference versus frequency at the detected Doppler channel k_{peak}. The altitude (R) is calculated by MUSIC algorism after compensating the phase shift due to the time difference of frequency steps. The compensation of the phase shift is described as

$$F(n,k_{peak}) = E(n,k_{peak})\exp\left[-j\left(\left(2\pi\frac{k_{peak}}{MN}\right)\cdot n\right)\right]$$
$$= A_{peak}\exp\left[j\left(\left(-\frac{4\pi\Delta f}{c}R\right)\cdot n - \frac{4\pi f_0 R}{c} + \pi f_d T_{PRI}\right)\right] \equiv A_{peak}\exp\left[j\varphi(n,k_{peak})\right]. \cdots\cdots\cdots (11)$$

For applying MUSIC algorism to calculate the altitude in multiple target situations, the correlation matrix of every frequency is averaged to recover the rank of the correlation matrix. Since difference of velocity between targets is continuous values, 5 data vectors, $F(n,k_{peak-2})$, $F(n,k_{peak-1})$, $F(n,k_{peak})$, $F(n,k_{peak+1})$, $F(n,k_{peak+2})$, around k_{peak} are employed for the procedure. The matrix $\mathbf{F}$ is composed of the

data vectors. The sub-matrix $\mathbf{F}_q$ that is composed of Ns rows of **F** is denoted by

$$\mathbf{F}_q \equiv submatrix\left[\mathbf{F}; n = q, q + Ns - 1, k = k_{peak} - 2, k_{peak} + 2\right] \in C^{Ns\times 5}$$
$$(q = 0, 1, \cdots, N - Ns), \cdots\cdots\cdots\cdots\cdots\cdots\cdots\cdots\cdots\cdots (12)$$

where $submatrix\,[\mathbf{A}; n = a, b, k = c, d]$ means sub-matrix that has rows from a to b and columns from c to d of **A** and N/2 is employed for the number of Ns. The correlation matrix is obtained by ensemble-averaging sub correlation matrix is written by

$$\mathbf{R} \equiv \left\langle \mathbf{F}_q \mathbf{F}_q^H \right\rangle \in C^{N_S\times N_S}, \cdots\cdots\cdots\cdots\cdots\cdots\cdots\cdots (13)$$

where $^{\mathrm{H}}$ and $\langle * \rangle$ denote the complex conjugate transpose of a matrix and ensemble-averaging. Then MUSIC algorithm is applied on **R**. The MUSIC spectrum is computed by performing an eigen-analysis on **R**. The space spanned by eigenvectors consists of two disjoint subspaces, which are signal and noise subspaces. In general, the larger and smaller eigenvalues belong to the signal and noise subspaces, respectively. The noise subspace is given by

$$\mathbf{E} = [\mathbf{e_1}, \mathbf{e_2}, \cdots \mathbf{e}_{\mathbf{N_s}-L}], \cdots\cdots\cdots\cdots\cdots\cdots\cdots\cdots (14)$$

where L is the number of signals (up to $Ns - 1$), which is determined by the eigenvalues of R. We assume that the number of signal components that cannot be separated by Doppler estimation is up to 3. In the situation where many signal components exist even after the Doppler estimation, the size of the data vector must be increased, which means increasing the number of frequency step N. One is the signal component from just below the airframe. The others are that from surrounding area. The steering vector to search the altitude is

$$\mathbf{a}(R) \equiv \exp\left[j\left(\left(-\frac{4\pi\Delta f}{c}R\right)\cdot n\right)\right] \in C^{N_s\times 1}. \cdots\cdots\cdots (15)$$

In terms of the orthogonal characteristics of eigenvectors in the signal and noise subspaces, the MUSIC spectrum is given by the following equation

$$MUSIC(R) = \frac{\mathbf{a}^H(R)\mathbf{a}(R)}{\mathbf{a}^H(R)\mathbf{E}\mathbf{E}^H\mathbf{a}(R)}. \cdots\cdots\cdots\cdots\cdots\cdots (16)$$

The range corresponding to the reflected wave from just below the airframe, which is altitude, is smaller than other ranges corresponding to the reflected waves from surrounding area. When MUSIC spectrum involves multiple range components, the minimum range where the amplitude exceeds a given threshold level and takes the local maximum value is assumed to be associated with the relative range between the airframe and the ground. In this method, the threshold is set to 60 dB lower than the maximum value.

2.3 Multiple Frequency CW Method with 2D MUSIC

The multiple frequency CW with 1D MUSIC consists of the velocity detection procedure by FFT and the altitude estimation procedure by MUSIC algorism described above. In the situation discussed in this paper, the relative velocities between the targets as well as ranges between targets are very close, thus high velocity resolution is also required. In this section, we describe the velocity and altitude estimation method based on 2D MUSIC algorism [6]. Multiple frequency CW with 2D MUSIC is expected to make it possible to achieve high range resolution and high velocity resolution. That means the method is expected to distinguish the targets having very close relative velocities and ranges. The observed signal is also expressed by Eq. (6). The matrix **F** is composed of linear arrays of m and n directions of observed signal as shown in Fig. 2.

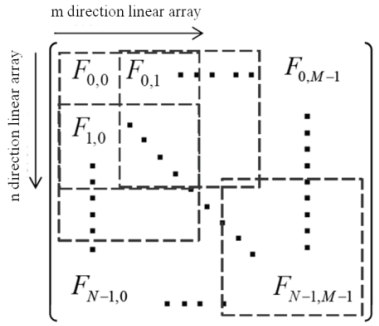

Fig. 2. Matrix element of **F** that is composed of linear arrays of m and n directions of observed signal and the extraction of sub-matrix

For applying MUSIC to estimate the velocity and altitude in the multiple target situations, the correlation matrix of every frequency is averaged to recover the rank of the correlation matrix as in the case with 1D MUSIC. The sub-matrix $\mathbf{F}_{\mathrm{q,p}}$ that composed of Nq rows and Np columns of **F** is denoted by

$$\mathbf{F}_{q,p} \equiv submatrix\,[\mathbf{F}; n = q, q + Nq - 1, m = p, p + Np - 1] \in C^{Nq\times Np}$$
$$(q = 0, 1, \cdots, N - Nq), (p = 0, 1, \cdots M - Np). \cdots\cdots (17)$$

Then the row vector is generated by rearranging the column vectors as

$$\mathbf{F}vec_{q,p} \equiv \left[\mathbf{F}^{\langle 1\rangle}(q,p)^T\mathbf{F}^{\langle 2\rangle}(q,p)^T\cdots\mathbf{F}^{\langle ,Np\rangle}(q,p)^T\right]^T \in C^{(Nq\cdot Np)\times 1}.$$
$$\cdots\cdots\cdots\cdots\cdots\cdots (18)$$

The correlation matrix is obtained by ensemble-averaging sub correlation matrix, which is written by

$$\mathbf{R} \equiv \left\langle \mathbf{F}vec_{q,p}\mathbf{F}vec_{q,p}^H \right\rangle \in C^{(N_q\cdot N_p)\times(N_q\cdot N_p)}.$$
$$= \frac{1}{(M - Np + 1)(N - Nq + 1)}\sum_{p=0}^{M-Np}\sum_{q=0}^{N-Nq}\mathbf{F}vec_{q,p}\mathbf{F}vec_{q,p}^H \in C^{(N_q\cdot N_p)\times(N_q\cdot N_p)}.$$
$$\cdots\cdots\cdots\cdots\cdots\cdots (19)$$

The MUSIC spectrum is computed by performing an eigen-analysis on **R** as in the case of 1D MUSIC. The noise subspace is given by

$$\mathbf{E} = [\mathbf{e_1}, \mathbf{e_2}, \cdots \mathbf{e}_{NqNp-L}], \cdots\cdots\cdots\cdots\cdots\cdots\cdots\cdots (20)$$

where L is the number of signals (up to $NqNp - 1$), which is determined by the eigenvalues of R. The size of data vector (Np × Nq) must be larger than the number of signals. On the other hand, the size of data vector is desirable to be small in terms of the computation load in the eigenvalue analysis and null search of MUSIC. In this research, we employ 48 for the size of data vector (Np = 8, Nq = 6). The *i*th element of steering vector $\mathbf{a}(R, V)$ to search the target range and relative

velocity is

$$a_i(R,V) \equiv \exp\left(j\left(2\pi\left(\frac{-2\Delta f}{c}R \bmod (i,Nq) + \frac{2V}{\lambda}NT_{pri}\cdot\frac{(i-\bmod(i,Np))}{Np}\right)\right)\right) \in C^{(Nq\cdot Np)\times 1}, \quad \cdots\cdots (21)$$

where mod(x, y) is an operator calculating a remainder of x/y.

The MUSIC spectrum is also given by the following equation

$$MUSIC(R,V) = \frac{\mathbf{a}^H(R,V)\mathbf{a}(R,V)}{\mathbf{a}^H(R,V)\mathbf{E}\mathbf{E}^H\mathbf{a}(R,V)}. \quad \cdots\cdots (22)$$

The MUSIC spectrum is possible to involve multiple peaks corresponding to the reflected waves from the ground just below the airframe and surrounding area. The range corresponding to the reflected wave from the ground directly below the airframe is assumed to take smaller value than that associated with the reflected waves from surrounding area. We detect the peak that takes the smallest range and regard it as the altitude of the airframe.

3. Evaluation on the Simulation Results

3.1 Ground Simulator used in This Research

A simulator to study the capability of altitude measurement of the multiple frequency CW radar in the situation where there are many reflection points is constructed. Tables 1, 2, and 3 show the radar parameters, airframe, and ground conditions, respectively. We conduct feasibility study on the multiple frequency CW for landing radar in the final phase of landing of exploration spacecrafts that is descending right down. The descending speed of the spacecraft in the final phase is assumed to be 1 m/s. It is reported that the pulse radar can measure the altitude from 3.5 km to 10 m [3]. In this research, we conduct simulation on the final phase of landing below the altitude of 10 m. The reflected power from each reflected point is expressed by the Eq. (23)

$$\Pr \propto \frac{G(\theta)^2\cdot\lambda^2\cdot\sigma(\theta)\cdot s\cdot\cos(\theta)}{(4\pi)^3\cdot R^4}, \quad \cdots\cdots (23)$$

$$E_n(t) = \sqrt{P_r}L_n \exp\left[j\left(2\pi\left(f_n + f_{d,n}\right)t - \frac{4\pi f_n}{c}R + \phi_n\right)\right], \quad \cdots\cdots (24)$$

where G is antenna gain. λ is the wave length. s is the size of one mesh. σ is backward scattering coefficient. θ is incident angle of the transmitted wave to the ground. In this simulation, we adopt Chebyshev beam pattern for antenna beam directionality [7].

The reflected signal is given by linear summation of the Eq. (2) from all reflected points on the ground. Individual amplitude of reflected signal is assumed to follow a Rayleigh distribution, which corresponds to L_n in Eq. (24) [8][9]. Same level of Gaussian noise is added on all altitude situations. In this condition, the S/N ratio is 30 dB when the radar is located at altitude of 3 m. The backscatter coefficient depends on the incident angles [10]. As described in chapter 2, we can assume following things. The step frequency bandwidth (Δf) is negligible small compared to the carrier frequency (Δf_0). The phase shift depending on the incident angle can be also ignored. The phase shift from each reflection point depends on only the path differences. Figure 3 shows an example of mappings of received power in the situation where the airframe is located at an altitude of 9 m.

Table 1. Radar parameters used in this research

Radar Parameters	Specification
Transmission Frequency	24.1125GHz
Number of Frequency Step	8
Sampling Rate	20kHz
Frequency Step Width/Maximum Range	10MHz/15m
Switching Time of Frequency/Maximum Velocity	50μs/7.8ms^{-1}
Observation Time/Velocity Resolution	102.4ms/0.06ms^{-1}
Antenna Beam Width	30deg(Chebyshev Pattern)
Transmission Power	10mW

Table 2. Conditions of the airframe on the simulation

Parameters	Setting Values
Altitude for Estimation	3-9m
Descending Velocity	1m/s

Table 3. Ground parameters on the simulation

Parameters on the Reflection (Ground)	Specification
Distribution of Surface Asperity	Uniform Distribution (0m - 0.028m)
Distribution of Reflection Intensity	Rayleigh Distribution
Backscatter Coefficient	Depending on the incident angle
Distance Decay	R^{-4}
Resolution of the Reflection	0.1m square
Simulated Area	10m square

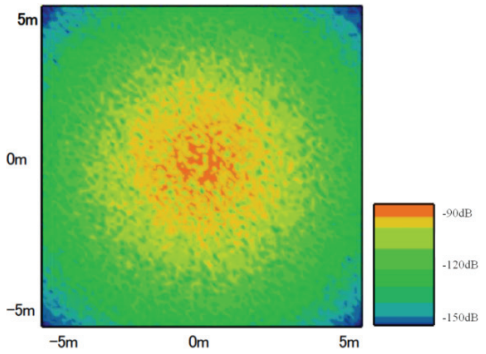

Fig. 3. Ground map of mean amplitude of received power from reflection points in the situation where the radar is located at the altitude of 9 m

3.2 Evaluation of the Basic Performance

At first, the situation where the airframe descends to the ground with the velocity of 1 m/s at an altitude of 9 m is simulated to evaluate the basic performance of the multiple frequency CW with 1D and 2D MUSIC.

Figure 4(a) shows $|E(n,k)|$ obtained by the signal processing for the target velocity of the multiple frequency CW with 1D MUSIC. The received signal from the ground just below the airframe is considered to have the maximum Doppler frequency. Thus the maximum frequency where the amplitude take the local maximum value and exceeds the threshold level as shown by a dash line in Fig. 4(a) is associated with the relative velocity 0between the airframe and the ground. The corresponding frequency is indicated by an arrow in Fig. 4(a). Figure 4(b) shows the MUSIC spectrum obtained by the signal processing for the altitude estimation using 1D MUSIC (Eq. (16)). As shown by an arrow in the figure, the minimum range where the amplitude takes local maximum value is the altitude of the airframe. The simulation is conducted 1000 times for obtaining statistical analysis results. Figure 5(a)

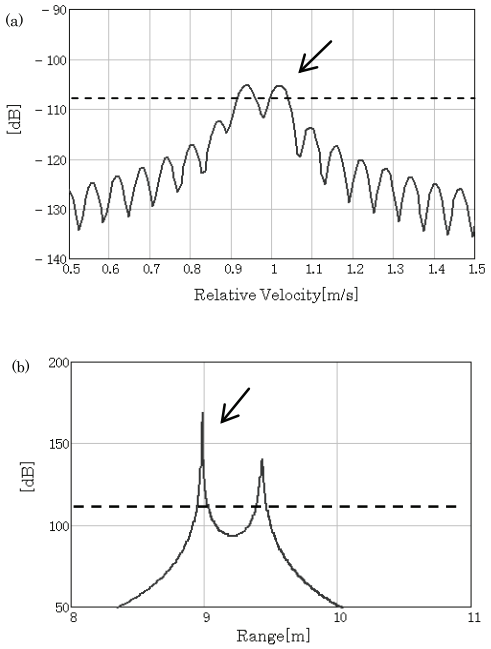

Fig. 4. Altitude estimation result at 9 m using multiple frequency CW with 1D MUSIC ((a) velocity estimation, (b) altitude esitimaion)

shows the histogram of altitude estimations calculated by the multiple frequency CW with 1D MUSIC. The mean and standard deviation of estimated altitude are 9.07 and 0.13, respectively. Simulations for the altitude between 3 m and 9 m are also conducted to investigate the dependency on altitude of the estimation results. Table 4 shows the mean value of the estimated altitude and the standard deviation at each altitude. The bias and random errors tend to decrease with decreasing altitude. The bias errors are less than 1% of the altitudes and the random errors are 1.3%–1.7% in the simulation.

Figure 6 shows an example of the spectrum obtained by 2D MUSIC (equation (20)) for the situation where the airframe descends to the ground with the velocity of 1 m/s at an altitude of 9 m. In Fig. 6, two peaks as indicated by arrows are identified. The one is located at velocity of 0.94 m/s, which is considered to be due to the reflected waves from the surrounding area. The other is located at velocity of 1.00 m/s, which is considered to be due to the reflected wave from just below the airframe. The estimated altitude is also calculated as 9.00 m. Among the spectrum peaks, the minimum range having spectrum peak is assumed to be the altitude of the airframe as described in chapter 2. As in the case of 1D MUSIC, the simulation is conducted 1000 times for obtaining statistical analysis results. Figure 5(b) shows the histogram of altitude estimations calculated by multiple frequency CW with 2D MUSIC for the situation where the airframe is located at an altitude of 9 m. The mean and standard deviation are 9.04 and 0.08, respectively. As in the case of 1D MUSIC, the simulations are also conducted between 3 m and 9 m. Table 5 shows the mean value of estimated altitude and standard deviation at each altitude. The bias errors are less than 1% of the altitudes and the random errors are limited to only 0.8%–1.0% in the simulation. In the application of landing radar for exploration spacecrafts in the final phase of landing, required accuracy for altitude measurement is 5% or 0.1 m of the altitude [3].

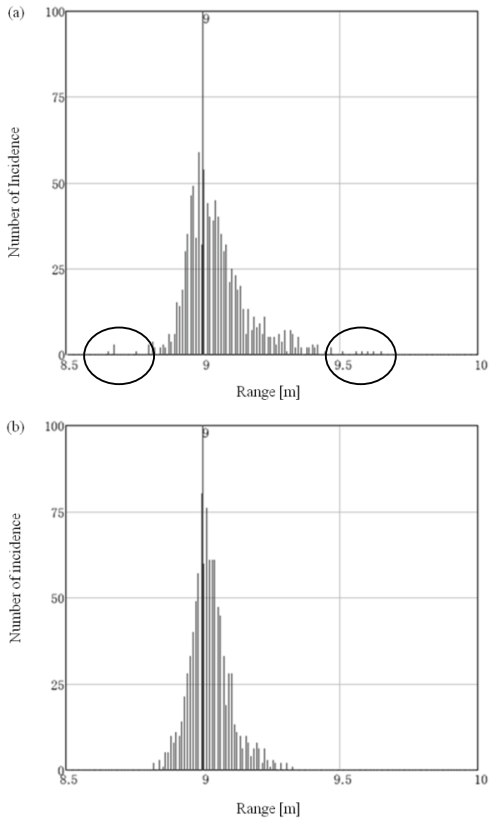

Fig. 5. Altitude estimation result at 9 m using multiple frequency CW ((a) with 1D MUSIC, (b) with 2D MUSIC)

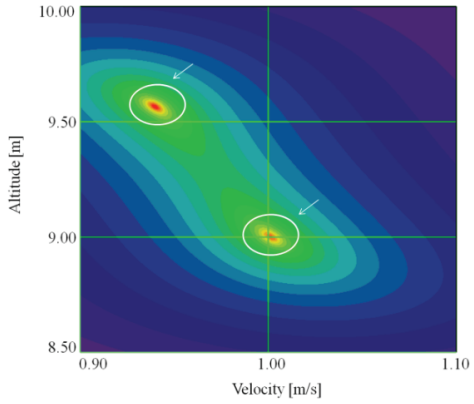

Fig. 6. Altitude estimation result at 9 m using multiple frequency CW with 2D MUSIC

Table 4. Simulation results of altitude estimation from the altitude of 3.0 m to 9.0 m with 1D MUSIC

Altitude	3	4	5	6	7	8	9
Mean value [m]	2.98	4	5.01	6.03	7.04	8.05	9.07
Standard deviation [m]	0.05(1.7%)	0.06(1.5%)	0.07(1.4%)	0.08(1.3%)	0.11(1.6%)	0.12(1.5%)	0.13(1.4%)

Table 5. Simulation results of altitude estimation from the altitude of 3.0 m to 9.0 m with 2D MUSIC

Altitude	3	4	5	6	7	8	9
Mean value [m]	2.97	3.98	4.99	6.01	7.02	8.03	9.04
Standard deviation [m]	0.03(1.0%)	0.04(1.0%)	0.04(0.8%)	0.05(0.8%)	0.06(0.9%)	0.07(0.9%)	0.08(0.9%)

4. Evaluation on Experimental Results

In this chapter, we show the fundamental experimental

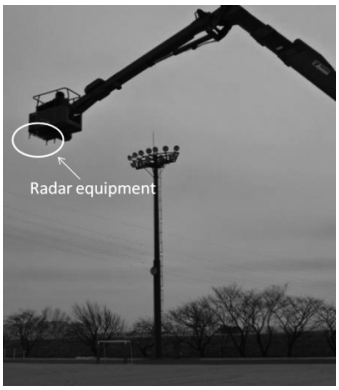

Fig. 7. Overview of the experiment on an athletic field

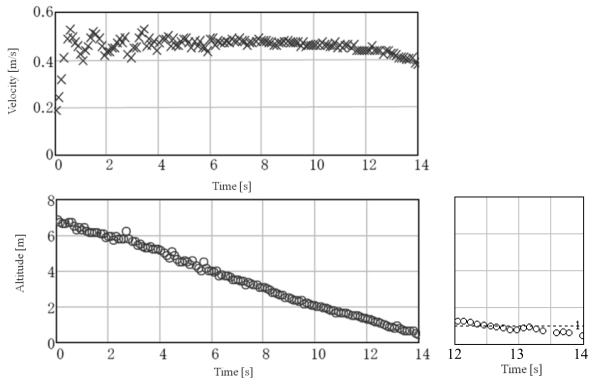

Fig. 8. Estimation results of velocity and altitude of the cage by multiple frequency CW with 1D MUSIC

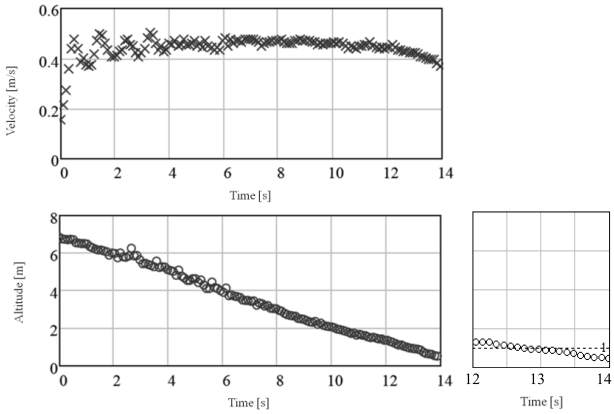

Fig. 9. Estimation results of velocity and altitude of the cage by multiple frequency CW with 2D MUSIC

results of the altitude measurement using multiple frequency CW radar on an athletic ground. Figure 7 shows the overview of the experiment using 24 GHz compact radar. In the experiment on the athletic ground, the radar is equipped on the cage of the crane as shown by a circle in Fig. 7. The radar beam is directed to the ground. Radar parameters are the same with the values adopted in the simulation described in chapter 3. The output waveform of radar is recorded by an A/D converter at the sampling rate of 20 kHz. The data is processed by the signal processing of multiple frequency CW with 1D and 2D MUSIC. Figures 8 and 9 show the results for the velocity and the altitude of the radar. The result indicates that the cage is initiated at the speed of 0.2 m/s and then descends to the ground at the speed of 0.4–0.5 m/s. Figures 8 and 9 also indicate that the radar can measure the altitude between 1.0 m and 7.0 m. We note that the random errors of 2D MUSIC are slightly smaller than those of 1D MUSIC. That is noticeable especially in low altitude as shown in the enlarged view from the time of 12 s to 14 s in Figs. 8 and 9. The observed signal that is composed of the reflected waves from reflection points on the ground involves the close Doppler frequency components and phase difference. 2D MUSIC seems to work well to distinguish the spectrum peaks associated with the reflected wave from the ground just below the airframe and associated with the reflected waves from the surrounding area. As a result of experiments, it is demonstrated that the velocity and altitude could be obtained by the compact radar equipped on the case of the crane with low sampling rate of 20 kHz using multiple frequency CW radar.

5. Discussion and Summary

In this paper, we conducted feasibility study on multiple Frequency CW for landing radar of spacecraft. We described the methods of multiple frequency CW with 1D and 2D MUSIC to measure the altitude of an airframe. Then we showed the simulation results using the ground simulator for the situation where the radar is equipped on an airframe that descending to the ground. We also showed the fundamental experimental results conducted on an athletic field using small radar equipped on a cage lifted by a crane.

As shown in the simulation section, the bias errors are less than 1% of the altitudes. The random errors of 1D MUSIC and 2D MUSIC are 1.3%–1.7% and 0.8%–1.0%, respectively. The bias and random errors tend to decrease with the decreasing altitude in the cases of 1D MUSIC and 2D MUSIC, which is considered to be due to S/N ratio. The random errors of 2D MUSIC are smaller than that of 1D MUSIC. We can also see that the bias error is not simply decreasing with altitude. In the simulation, the size of reflection point is limited to 0.1 m square because of the computation load. Thus the size limitation is considered to affect the simulation result especially in the low altitude. The bias error of 3 cm in low altitude is also considered to be enough small compared to the required performance.

In the histogram of 1D MUSIC, some estimation results having far different values from the altitude are identified as indicated by circles in Fig. 5(a). In these cases, wrong velocities were chosen by the target detection procedure. The Doppler velocity associated with the reflected wave from just below the airframe does not always take maximum amplitude as shown in Fig. 4. These amplitudes are sometimes smaller than 3 dB from the maximum value. On the other hand, such far different values from the altitude were not identified in the histogram of 2D MUSIC in Fig. 5(b). Also, multiple frequency CW with 2D MUSIC satisfied the required performance of landing radar in the final phase. On the experiment on the athletic field, stable estimation results on altitude are obtained from the initiation to the end. The experimental result also indicates that the random error of 2D MUSIC is slightly smaller than that of 1D MUSIC.

These results indicated that multiple frequency CW was one of the effective tools for landing radar in the final phase of landing. The fundamental experiment was conducted on

the good weather condition with no dust, since we concentrated on the fundamental capability of the method for estimating altitude. Further research including experiments on the situation with dense dust is also needed.

References

(1) M. Rangwala, F. Wang, and K. Srabandi: "Study of Millimeter-Wave Radar for Helicopter Assisted-Landing System", IEEE Antennas and Propagation Magazine, Vol.50, No.2, pp.13–25 (2008)

(2) T. Sato, T. Sakai, S. Fukuda, and T. Mizuno: "Study on Terrain Dependence of a C-Band Pulse Doppler Radar for Lunar Landar", IEICE Technical Report SANE, Vol.107, No.407, pp.19–24 (2007)

(3) S. Fukuda, T. Mizuno, T. Sakai, H. Tomita, and H. Ishimaru: "Development of the C-Band Pulse Radar for Lunar/Planetary Landers", IEICE Technical Report SANE, Vol.104, No.469, pp.7–12 (2004)

(4) T. Inaba: "Multiple Target Detection for Stepped Multiple Frequency Interrupted CW Radar", IEICE Transactions on Communications, Vol.J89-B, No.3, pp.373–383 (2006)

(5) T. Watanabe, R. Yamashita, and T. Inaba: "Multiple Frequency CW Radar using Two Initial Frequencies", IEICE Technical Report SANE, Vol.112, No.391, pp.19–24 (2013)

(6) T. Inaba and F. Fukushima: "Super Resolution Range/Angle Estimation Using Stepped Multiple Frequency Interrupted CW Radar", IEICE Transactions on Communications, Vol.J91-B, No.7, pp.756–767 (2008)

(7) C.L. Dolph: "A current distribution for broadside arrays which optimizes the relationship between beam width and side-lobe level", Proc. of the I.R.E. and Waves and Electrons, pp.335–348 (1946)

(8) S. Sayama and S. Matsuo: "Amplitude Statistics of Ground Clutter Included Town Using a Millimeter Wave Radar", IEICE Transactions on Communications, Vol.J86-B, No.5, pp.829–836 (2003)

(9) I. Matsunami, Y. Nakahata, K. Ono, amd A. Kajiwara: "Clutter Characteristics by UWB Radar at 24 GHz Band", IEICE Transactions on Communications, Vol.J92-B, No.1, pp.363–366 (2009)

(10) F. T.Ulaby and M. Dobson: "HANDBOOK of Radar Scattering Statistics for Terrain", Artech House, Boston (1989)

Manabu Akita (Member) received the B.S. in Communications Engineering and the M.S. and the Ph.D. in Electrical, Electronic and Information Engineering from Osaka University in 2005, 2008 and 2011, respectively. After he was a research fellow of the Japan Society for the Promotion of Science (JSPS Research Fellow) from 2010 to 2011, he joined New Mexico Institute of Mining and Technology where he was an postdoctral research fellow in 2012. In 2013, he joined the Department of Mechanical Engineering and Intelligent Systems, University of Electro-Communications where he was an assistant professor. His main interests are in remote sensing and measurement engineering.

Daisuke Nakashima (Non-member) received the B.E. from the University of Electro-Communications in 2011 and the M.E. degree from University of Electro-Communications in 2013.

Masato Watanabe (Non-member) received B.E. from the University of Electro-Communications and M.E. from University of Electro-Communications in 2009 and 2011. Currently, he is a Research fellow of the University of Electro-Communications in engineering from University of Electro-Communications. His main interest is in radar signal processing.

Takayuki Inaba (Non-member) received a B.S. degree from the Department of Physics, Tokyo Institute of Technology, in 1981, completed the M.E. program in physics in 1983. He received the Ph.D. degree in engineering from Tokyo Institute of Technology in 2001. He joined the Department of Mechanical Engineering and Intelligent Systems, University of Electro-Communications where he was a professor. He is engaged in research on radar signal processing, and signal processing for adaptive arrays and automotive radars.